METALLURGY OF NON-FERROUS METALS / МЕТАЛЛУРГИЯ ЦВЕТНЫХ МЕТАЛЛОВ

UDC 66.083.3
https://doi.org/10.17073/0021-3438-2025-3-16-27

Research article
Научная статья

Optimization of low-temperature sulfuric acid leaching of chalcopyrite and pyrite

M.A. Tretiak, K.A. Karimov, U.R. Sharipova, A.V. Kritskiy, D.A. Rogozhnikov

Ural Federal University n.a. the First President of Russia B.N. Yeltsin
19 Mira Str., Ekaterinburg 620002, Russia

✉ Maksim A. Tretiak (m.a.tretiak@urfu.ru)

Abstract: This study presents the results of oxidative leaching of chalcopyrite ($CuFeS_2$) and pyrite (FeS_2) in a sulfuric acid medium at low temperature in the presence of copper (Cu^{2+}) and iron (Fe^{3+}) ions. Using orthogonal experimental design, the optimal conditions were identified to maximize sulfide matrix decomposition and valuable metal recovery. Experiments were conducted at a constant temperature of 100 °C. The parameters investigated included partial oxygen pressure (0.2–0.75 MPa), concentrations of sulfuric acid (10–50 g/dm^3), Fe^{3+} ions (2–10 g/dm^3), Cu^{2+} ions (1–3 g/dm^3), and leaching time (60–240 min). The composition of the feed minerals and leach products was analyzed by *X*-ray fluorescence (XRF) analysis, *X*-ray diffraction (XRD) analysis, and atomic absorption spectrometry (AAS). Maximum copper recovery from chalcopyrite (55 %) was achieved under the following conditions: O_2 partial pressure of 0.25 MPa, initial concentrations of H_2SO_4 – 50 g/dm^3, Cu^{2+} – 1 g/dm^3, Fe^{3+} – 2.5 g/dm^3, and leaching time – 240 min. The maximum degree of pyrite oxidation (56 %) was obtained at an O_2 partial pressure of 0.75 MPa, initial concentrations of H_2SO_4 – 50 g/dm^3, Cu^{2+} – 2 g/dm^3, and Fe^{3+} – 10 g/dm^3. The results showed that leaching time and oxygen pressure have the greatest effect on chalcopyrite and pyrite decomposition ($p < 0.05$). The interaction between Fe^{3+} and Cu^{2+} ions was also established: excess Fe^{3+} (>10 g/dm^3) leads to hydrolysis and decreases chalcopyrite leaching efficiency, whereas Cu^{2+} promotes partial formation of secondary copper sulfides. Regression equations ($R^2 = 0.98$ for chalcopyrite and $R^2 = 0.96$ for pyrite) were derived, providing an adequate description of the process.

Keywords: chalcopyrite, pyrite, copper, iron, autoclave, autoclave leaching, sulfuric acid, oxygen.

Acknowledgments: The research was supported by the Russian Science Foundation (Project No. 25-29-00838, https://rscf.ru/project/25-29-00838/).

For citation: Tretiak M.A., Karimov K.A., Sharipova U.R., Kritskiy A.V., Rogozhnikov D.A. Optimization of low-temperature sulfuric acid leaching of chalcopyrite and pyrite. *Izvestiya. Non-Ferrous Metallurgy*. 2025;31(3):16–27.
https://doi.org/10.17073/0021-3438-2025-3-16-27

Оптимизация процессов низкотемпературного серно-кислотного выщелачивания халькопирита и пирита

М.А. Третьяк, К.А. Каримов, У.Р. Шарипова, А.В. Крицкий, Д.А. Рогожников

Уральский федеральный университет имени первого Президента России Б.Н. Ельцина
Россия, 620002, г. Екатеринбург, ул. Мира, 19

✉ Максим Алексеевич Третьяк (m.a.tretiak@urfu.ru)

Аннотация: В работе представлены результаты исследования процессов окислительного выщелачивания халькопирита ($CuFeS_2$) и пирита (FeS_2) в серно-кислой среде при низких температурах с добавлением ионов меди (Cu^{2+}) и железа (Fe^{3+}). Методом ортогонального планирования эксперимента установлены оптимальные условия процесса, обеспечивающие максимальную степень

деструкции сульфидной матрицы и извлечение ценных металлов. Эксперименты проводились при постоянной температуре 100 °С. Исследовались следующие параметры: парциальное давление кислорода (0,2–0,75 МПа), концентрации серной кислоты (10–50 г/дм^3), ионов Fe^{3+} (2–10 г/дм^3) и Cu^{2+} (1–3 г/дм^3), а также продолжительность процесса (60–240 мин). Состав исходных минералов и продуктов выщелачивания анализировали методами рентгеноспектрального флуоресцентного анализа, рентгенофазового анализа и атомно-абсорбционной спектрометрии. Установлено, что максимальное извлечение меди из халькопирита (55 %) достигается при следующих условиях: парциальном давлении O_2 – 0,25 МПа, исходных концентрациях H_2SO_4 – 50 г/дм^3, Cu^{2+} – 1 г/дм^3, Fe^{3+} – 2,5 г/дм^3, продолжительности процесса – 240 мин. Максимальная степень окисления пирита составила 56 % при парциальном давлении кислорода 0,75 МПа, исходных концентрациях H_2SO_4 – 50 г/дм^3, Cu^{2+} – 2 г/дм^3 и Fe^{3+} – 10 г/дм^3. Установлено, что продолжительность и давление кислорода оказывают наиболее значимое влияние на степень разложения халькопирита и пирита ($p < 0,05$). Выявлены особенности взаимодействия ионов Fe^{3+} и Cu^{2+}: избыток Fe^{3+} (>10 г/дм^3) приводит к гидролизу и снижению эффективности выщелачивания халькопирита, тогда как Cu^{2+} способствует частичному образованию вторичных сульфидов меди. Выведены уравнения регрессии ($R^2 = 0,98$ для халькопирита и $R^2 = 0,96$ для пирита), адекватно описывающие процесс.

Ключевые слова: халькопирит, пирит, медь, железо, автоклав, выщелачивание, серная кислота, кислород.

Благодарности: Исследование выполнено за счет гранта Российского научного фонда № 25-29-00838, https://rscf.ru/project/25-29-00838/

Для цитирования: Третьяк М.А., Каримов К.А., Шарипова У.Р., Крицкий А.В., Рогожников Д.А. Оптимизация процессов низкотемпературного серно-кислотного выщелачивания халькопирита и пирита. *Известия вузов. Цветная металлургия.* 2025;31(3):16–27. https://doi.org/10.17073/0021-3438-2025-3-16-27

Introduction

Sulfide minerals, particularly chalcopyrite ($CuFeS_2$) and pyrite (FeS_2), are of significant interest in modern hydrometallurgy as the main sources of non-ferrous and noble metals. However, their processing presents substantial technological challenges due to the high chemical stability of the sulfide matrix. Conventional pyrometallurgical methods are characterized by high energy consumption and the release of toxic gaseous emissions, which highlights the need for the development of more environmentally friendly and economically efficient hydrometallurgical technologies [1—3].

Recent trends in the hydrometallurgy of non-ferrous metals demonstrate growing interest in the creation of energy-efficient methods for processing sulfide raw materials [4—10].

In recent years, autoclave hydrometallurgy has seen a shift toward the development and implementation of low-temperature mineral processing techniques [11—14]. This direction is of particular scientific and practical interest, as it makes it possible to significantly optimize both technological and economic performance indicators. Conducting leaching processes at low temperatures (60—110 °C) under either atmospheric or autoclave conditions can reduce energy consumption, simplify process equipment, and enable the oxidation of sulfur predominantly to its elemental form compared to conventional high-temperature autoclave processes [15]. However, during oxidative leaching of sulfide minerals, the formation of elemental sulfur leads to the development of passivating layers on particle surfaces, which substantially slows down the reaction.

Modern approaches to addressing this issue involve a range of technological solutions that combine different process intensification methods. The most common techniques include preliminary mechanochemical activation in mills, which generates a defect-rich crystal structure, as well as the use of surfactants and catalytic additives (Ag^+, Cu^{2+}, Fe^{3+} ions) that destabilize sulfur films by modifying their morphology and increasing the porosity of the passivating layer [16—18]. Studies [19—21] have demonstrated that the addition of silver during chalcopyrite leaching with ferric sulfate solutions significantly enhances the leaching process, resulting in shorter leaching times and higher copper recovery into solution. The low rate of chalcopyrite oxidation by Fe^{3+} is attributed to the formation of a passivating elemental sulfur layer, which acts as a barrier to reagent access at the mineral surface. This interpretation is supported by studies [22; 23], which reported oxidation of sulfide concentrates containing chalcopyrite, sphalerite, and arsenopyrite in ferric-containing solutions in the presence of pyrite. The authors analyzed the kinetics and proposed a mechanism for the interaction of sulfide minerals with ferric ions and pyrite.

Experimental studies of the kinetics and mechanisms of chalcopyrite- and pyrite-containing material

oxidation under hydrothermal conditions, conducted since the 1950s, reveal considerable variation in reported results. These discrepancies arise from differences in the mineralogical and chemical composition of the feed, process conditions (temperature, oxygen pressure, pH, etc.), and methodological approaches to interpreting experimental data. Therefore, the study of sulfide raw material processing remains an important research objective, especially in view of advances in analytical methods and the evolving mineral composition of ores being processed.

In autoclave sulfuric acid leaching, the oxidation of $CuFeS_2$ and FeS_2 is described by the following principal reactions:

$$2CuFeS_2 + 2H_2SO_4 + 7O_2 = 2CuSO_4 + Fe_2(SO_4)_3 + S^0 + 2H_2O, \quad (1)$$

$$CuFeS_2 + H_2SO_4 + 2.5O_2 = CuSO_4 + FeSO_4 + S^0 + H_2O, \quad (2)$$

$$CuFeS_2 + 2Fe_2(SO_4)_3 = CuSO_4 + 5FeSO_4 + 2S^0, \quad (3)$$

$$CuFeS_2 + 4O_2 = CuSO_4 + FeSO_4, \quad (4)$$

$$5FeS_2 + 4H_2SO_4 + 4O_2 = 5FeSO_4 + 9S^0 + 4H_2O, \quad (5)$$

$$FeS_2 + 3.5O_2 + H_2O = FeSO_4 + H_2SO_4, \quad (6)$$

$$7FeS_2 + 4Fe_2(SO_4)_3 + 4H_2SO_4 = 14FeSO_4 + 14S^0 + 4H_2O, \quad (7)$$

$$4FeS_2 + 9O_2(g) + 4H_2SO_4 = 4\,Fe_2(SO_4)_3 + 8S^0 + 4H_2O, \quad (8)$$

$$4FeSO_4 + O_2(g) + 2H_2SO_4 = 2Fe_2(SO_4)_3 + 2H_2O. \quad (9)$$

These reactions show that sulfide sulfur in chalcopyrite may be oxidized by oxygen to elemental sulfur and sulfate ions (reactions (1)—(3)). Ferric ions can also act as oxidants, in which case sulfide sulfur is oxidized to the elemental state (reaction (4)), while ferrous ions react with oxygen to regenerate ferric ions.

Given the significance of this issue, the present study focuses on low-temperature oxidative autoclave leaching of chalcopyrite and pyrite in a sulfuric acid medium with copper (Cu^{2+}) and iron (Fe^{3+}) ions as catalytic additives. The main objective is to determine the optimal process parameters (temperature, partial oxygen pressure, sulfuric acid concentration, and catalytic additives) that ensure maximum recovery of non-ferrous metals.

Materials and methods

Chalcopyrite and pyrite from the Vorontsovskoye and Berezovskoye deposits (Sverdlovsk region, Russia), respectively, were used as the objects of study in low-temperature oxidative autoclave leaching. The chemical composition of the minerals (Table 1) was determined by *X*-ray fluorescence (XRF) analysis using an ED-XRF spectrometer (EDX-7000, Shimadzu, Japan).

Particle size distribution of the minerals was determined by laser diffraction using a Bettersize ST analyzer (Bettersize, China) (Fig. 1). The characteristic chalcopyrite particle sizes d_{10}, d_{50}, and d_{90} are 3.8, 28.8, and 79.9 μm, respectively. Analysis of the particle size distribution indicates that the predominant fraction of the sample lies within 30—90 μm. The wide gap between d_{10} and d_{90} (>76 μm) confirms a high degree of particle size heterogeneity.

For pyrite, the d_{10}, d_{50}, and d_{90} are 3.41, 14.81, and 53.77 μm, respectively. Differential distribution analysis shows that the main fraction was within 10—45 μm, accounting for more than 50 % of the sample.

The minerals were ground and sieved on laboratory screens, after which the working fraction was selected with 80 % passing ≤40 μm.

X-ray diffraction (XRD) analysis was performed using an XRD-7000 Maxima diffractometer (Shimadzu, Japan). Diffraction data were processed using Match!3 software with the PDF-2 database and the WWW-MINCRYST database of minerals and structural analogs. The results are shown in Fig. 2.

XRD analysis of the CuFeS2 and FeS2 samples showed minor peaks of silicon dioxide, with concentrations not exceeding 0.5 % in chalcopyrite and 5.1 % in pyrite.

To achieve the required initial concentrations of sulfuric acid, Cu^{2+}, and Fe^{3+} ions, analytical-grade rea-

Chemical composition of sulfide minerals

Химический состав сульфидных минералов

Mineral	Content, wt. %			
	Cu	Fe	S	Other
$CuFeS_2$	33.4	32.0	34.1	0.5
FeS_2	–	44.1	50.8	5.1

gents H_2SO_4, $CuSO_4 \cdot 5H_2O$, and $Fe_2(SO_4)_3 \cdot 9H_2O$ were used, dissolved in double-distilled water.

Statistical processing of results was carried out using Statgraphics 19 software with Microsoft Excel visualization tools. Chemical analysis of the leach products was performed by flame atomic absorption spectrometry (FAAS) on a NovAA 300 spectrometer (Analytik Jena, Germany). Classical titrimetric methods [24] were used to determine Fe^{2+} and residual H_2SO_4 concentrations in the solutions.

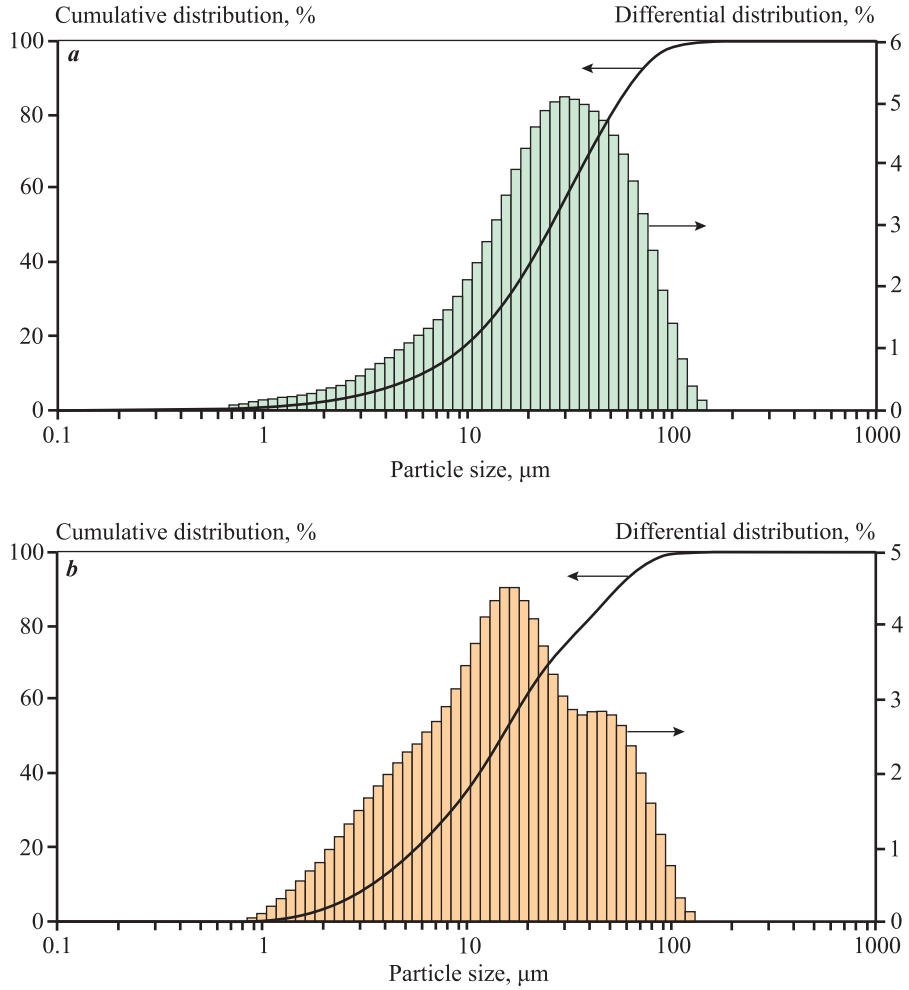

Fig. 1. Particle size distribution of chalcopyrite (***a***) and pyrite (***b***)

Рис. 1. Результаты гранулометрического анализа халькопирита (***a***) и пирита (***b***)

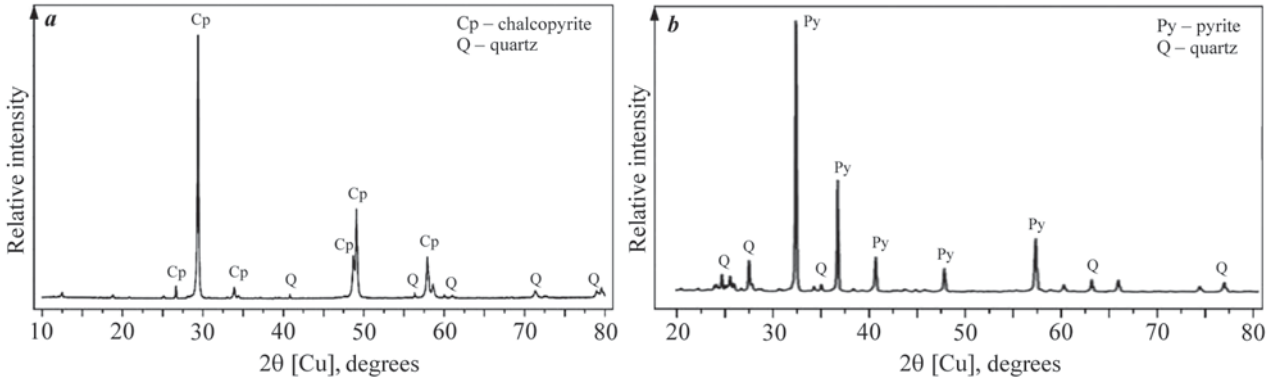

Fig. 2. XRD patterns of chalcopyrite (***a***) and pyrite (***b***)

Рис. 2. Дифрактограммы проб халькопирита (***a***) и пирита (***b***)

Leaching experiments were conducted in a sealed laboratory autoclave reactor system made of titanium alloy (Parr Instrument Company, USA), with a nominal volume of 1.0 dm^3 and a filling ratio of 0.6. The autoclave was equipped with a multifunctional monitoring system (temperature sensor, pressure sensor, and stirrer rotation speed sensor), a mixing mechanism (electromagnetic drive with variable speed control), and an oxygen flowmeter. A distinctive feature of the reactor was its ability to introduce reagents during operation without depressurization. Temperature control was provided by a two-section electric heating system connected to a digital PID controller, which maintained the set temperature within ±1 °C.

Before the experiment, a 20 g sulfide mineral sample was weighed on an analytical balance, and a 600 cm^3 solution containing the required concentrations of H_2SO_4, Fe^{3+}, and Cu^{2+} was prepared. After loading the slurry, the autoclave was sealed, stirring was started, and the pulp was heated to 100 °C. The stirring speed was maintained at 800 rpm. Once the target temperature was reached, oxygen was supplied and the experiment start time was recorded. At the end of the test, oxygen flow was stopped and the autoclave was cooled to 70 °C. The slurry was filtered, the residue washed, and dried to constant weight. Solid and liquid samples were then prepared for analysis.

Experimental studies were performed according to a second-order orthogonal design, including five variable factors at a fixed process temperature of 100 ± 1 °C, which prevents elemental sulfur melting. This temperature regime was selected as a constant parameter for all tests.

The independent variables were partial oxygen pressure (0.2—0.75 MPa), initial concentrations of sulfuric acid (10—50 g/dm^3), Fe^{3+} ions (2—10 g/dm^3), Cu^{2+} ions (1—3 g/dm^3), and leaching time (60—240 min). The dependent variables were copper and iron recoveries from chalcopyrite and pyrite, respectively.

Results and discussion

To assess the effect of copper and iron ions on chalcopyrite oxidation in a sulfuric acid medium, the degree of $CuFeS_2$ decomposition was plotted as a function of time (Fig. 3). In an earlier study [25], the kinetics of copper mineral dissolution, including $CuFeS_2$, were examined at low temperature and an oxygen pressure of 0.15—0.95 MPa, with a particle size of −0.44 μm (100 %).

As shown in Fig. 3, in the absence of sulfuric acid and ferric ions, chalcopyrite oxidation does not exceed 8 % after 240 min of leaching. In a weakly acidic medium ($[H_2SO_4]_0$ = 5 g/dm^3) [25], Fe^{2+} ions and covellite are formed according to

$$5CuFeS_2 + 3O_2 + 6H_2SO_4 = \\ = CuSO_4 + FeSO_4 + 4CuS + 6S^0 + 6H_2O, \quad (10)$$

which raises the degree of $CuFeS_2$ oxidation to 27 %.

When $[H_2SO_4]_0$ = 0 и $[Fe^{3+}]_0$ = 20 g/dm^3, the presence of Fe^{3+}, in accordance with the stoichiometric reaction (3), leads to the formation of ferrous sulfate and elemental sulfur. The low concentrations of H_2SO_4 (4.3 g/dm^3) and Fe^{2+} (3.5 g/dm^3) detected in the final solution indicate partial oxidation of sulfide sulfur to sulfate through

$$CuFeS_2 + Fe_2(SO_4)_3 + 3.5O_2 + H_2O = \\ = CuSO_4 + 3FeSO_4 + H_2SO_4, \quad (11)$$

thereby creating a weakly acidic medium that facilitates chalcopyrite oxidation via reactions (1) and (2), and Fe^{2+} oxidation to Fe^{3+} via reaction (9).

With an excess sulfuric acid concentration ($[H_2SO_4]_0$ = 50 g/dm^3) and the presence of Fe^{3+} ions, the degree of chalcopyrite dissolution increases to 35 %.

The addition of Cu_{2+} promotes the formation of secondary copper sulfides (CuS, Cu_2S) and makes it possible to reduce the initial $[Fe^{3+}]_0$ to <10 g/dm^3 due to the

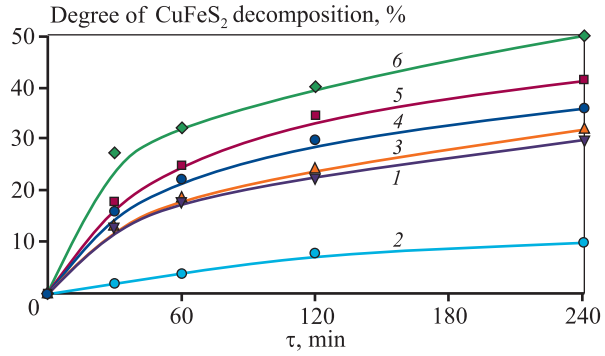

Fig. 3. Degree of $CuFeS_2$ decomposition vs. leaching time (P_{O_2} = 0.475 MPa)

Concentrations, g/dm^3: ***1*** – $[H_2SO_4]_0$ = 5, *t* = 110 °C, [25]; ***2*** – $[H_2SO_4]_0$ = 0, $[Fe^{3+}]_0$ = 0; ***3*** – $[H_2SO_4]_0$ = 50, $[Fe^{3+}]_0$ = 0; ***4*** – $[H_2SO_4]_0$ = 0, $[Fe^{3+}]_0$ = 20; ***5*** – $[H_2SO_4]_0$ = 50, $[Fe^{3+}]_0$ = 20; ***6*** – $[H_2SO_4]0$ = 50, $[Fe^{3+}]_0$ = 3,$[Cu^{2+}]_0$ = 2

Рис. 3. Степень разложения $CuFeS_2$ в зависимости от продолжительности эксперимента (P_{O_2} = 0,475 МПа)

Концентрации, г/$дм^3$: ***1*** – $[H_2SO_4]_0$ = 5, *t* = 110 °C, [25]; ***2*** – $[H_2SO_4]_0$ = 0, $[Fe^{3+}]_0$ = 0; ***3*** – $[H_2SO_4]_0$ = 50, $[Fe^{3+}]_0$ = 0; ***4*** – $[H_2SO_4]_0$ = 0, $[Fe^{3+}]_0$ = 20; ***5*** – $[H_2SO_4]_0$ = 50, $[Fe^{3+}]_0$ = 20; ***6*** – $[H_2SO_4]0$ = 50, $[Fe^{3+}]_0$ = 3,$[Cu^{2+}]_0$ = 2

formation and subsequent oxidation of $FeSO_4$ according to reactions (9), (12), and (13):

$$CuFeS_2 + CuSO_4 \rightarrow 2CuS + FeSO_4, \quad (12)$$

$$5CuFeS_2 + 11CuSO_4 + 8H_2O \rightarrow$$
$$\rightarrow 8Cu_2S + 5FeSO_4 + 8H_2SO_4. \quad (13)$$

Under these conditions, the degree of chalcopyrite decomposition reaches approximately 50 % within 240 min.

To determine the statistically significant parameters and evaluate their effect on chalcopyrite dissolution, a Pareto chart was constructed (Fig. 4).

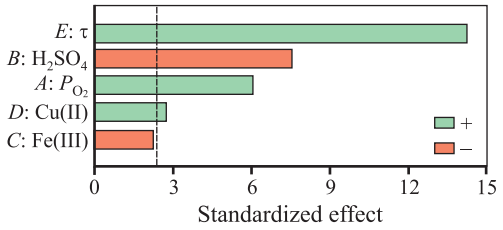

Fig. 4. Pareto chart for chalcopyrite oxidation

Рис. 4. Диаграмма Парето для окисления халькопирита

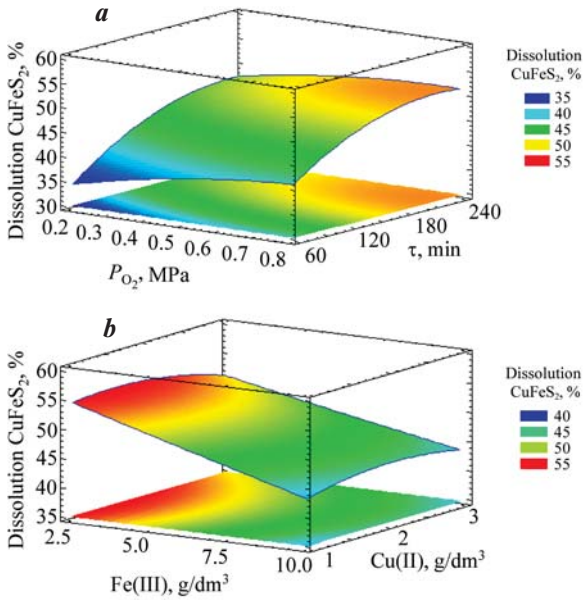

Fig. 5. Dependence of chalcopyrite dissolution on partial oxygen pressure and leaching time (***a***), and the initial concentrations of Cu^{2+} and Fe^{3+} ions (***b***)

Рис. 5. Зависимость растворения халькопирита от парциального давления кислорода и продолжительности опыта (***a***), а также от исходных концентраций ионов Cu^{2+} и Fe^{3+} (***b***)

Leaching time, initial sulfuric acid concentration, partial oxygen pressure, and Cu^{2+} concentration exert the strongest effects on chalcopyrite dissolution under low-temperature oxidative autoclave conditions.

Based on the experimental results, a three-dimensional response surface was generated to describe chalcopyrite dissolution as a function of partial oxygen pressure and leaching time at $[H_2SO_4]_0$ = = 31 g/dm^3, $[Cu^{2+}]_0$ = 2 g/dm^3, $[Fe^{3+}]_0$ = 6,25 g/dm^3 (Fig. 5, *a*).

As shown earlier, leaching time has the strongest positive effect on chalcopyrite dissolution. At P_{O_2} = = 0.6÷0.8 MPa and τ = 180 min, copper recovery reaches 50—55 %. Reducing the leaching time to 60 min results in a sharp decrease in copper recovery to 35—40 %.

Fig. 5, *b* illustrates the effects of Cu^{2+} and Fe^{3+} concentrations on chalcopyrite dissolution under constant conditions: $[H_2SO_4]_0$ = 50 g/dm^3, P_{O_2} = 0.475 MPa, τ = 240 min.

It was observed that increasing $[Fe^{3+}]_0$ from 2.5 to 10 g/dm^3 decreases copper recovery from 55 % to 44 %. This effect may be attributed to the accumulation of Fe^{3+} in solution, which promotes oxidation of $CuFeS_2$ to elemental sulfur via reaction (3), followed by sulfur passivation of the mineral particles [26; 27].

When the oxygen pressure is reduced to 0.2—0.4 MPa and the initial Fe^{3+} concentration to 2.5 g/dm^3 (Fig. 6), the contribution of reaction (9) — the generation and excess accumulation of Fe^{3+} — is limited, thereby reducing the likelihood of iron hydrolysis. Under these conditions, sulfuric-acid decomposition of chalcopyrite via reactions (1)—(4) proceeds with less restriction on reagent access to the mineral surface and remains at ~55 % after 240 min of leaching.

From the experimental data, the following regression equation was derived:

$$CuFeS_2 = 11.6514 + 2.55712P_{O_2} -$$
$$- 0.205448C_{H_2SO_4} + 0.319954C_{Fe(III)} +$$
$$+ 7.55577C_{Cu(II)} + 0.272454\tau - 0.130897P_{O_2} +$$
$$+ 0.00604642C_{H_2SO_4} + 0.00724245C^2_{Fe(III)} -$$
$$- 1.61708C^2_{Cu(II)} - 0.000451762\tau^2, \quad (14)$$

where P_{O_2} is the partial oxygen pressure, MPa; $C_{H_2SO_4}$, $C_{Fe(III)}$, $C_{Cu(II)}$ — are the initial concentrations of sulfuric acid, Fe^{3+}, and Cu^{2+} ions (g/dm^3), respectively; and τ is the leaching time (min).

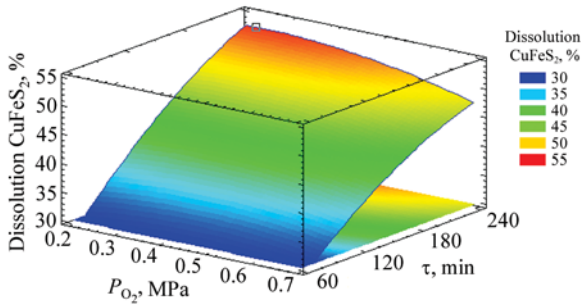

Fig. 6. Dependence of chalcopyrite dissolution on partial oxygen pressure and leaching time
$[H_2SO_4]_0$ – 50 g/dm^3, $[Cu^{2+}]_0$ – 1 g/dm^3, $[Fe^{3+}]_0$ – 2,5 g/dm^3

Рис. 6. Зависимость растворения халькопирита от парциального давления кислорода и продолжительности опыта
$[H_2SO_4]_0$ – 50 г/дм^3, $[Cu^{2+}]_0$ – 1 г/дм^3, $[Fe^{3+}]_0$ – 2,5 г/дм^3

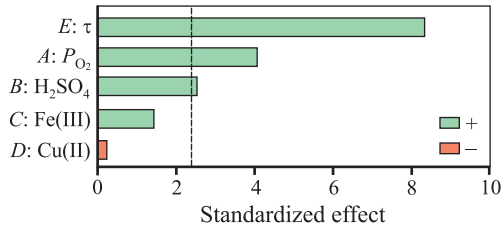

Fig. 7. Pareto chart for pyrite oxidation

Рис. 7. Диаграмма Парето для окисления пирита

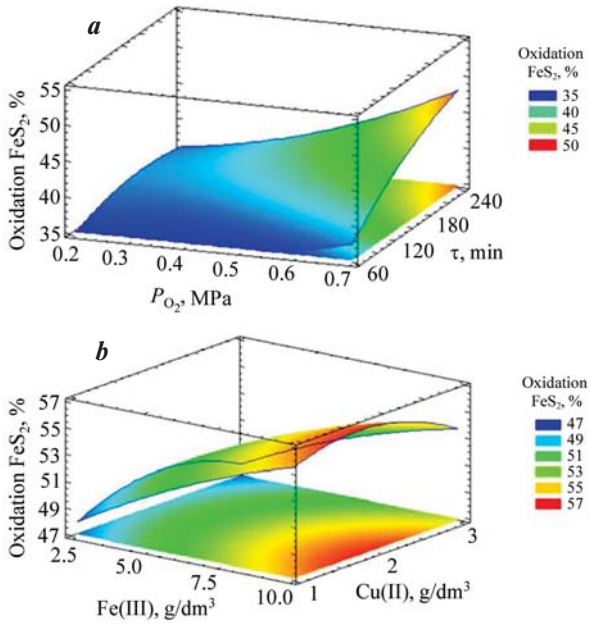

Fig. 8. Dependence of pyrite dissolution on partial oxygen pressure and leaching time (***a***), and initial concentrations of Cu^{2+} and Fe^{3+} ions (***b***)
a: $[H_2SO_4]_0$ – 31 g/dm^3, $[Cu^{2+}]_0$ – 2 g/dm^3, $[Fe^{3+}]_0$ – 6,25 g/dm^3
b: $[H_2SO_4]_0$ – 50 g/dm^3, P_{O_2} – 0,475 MPa, τ – 240 min

Рис. 8. Зависимость растворения пирита от парциального давления кислорода и продолжительности опыта (***a***), а также от исходных концентраций ионов Cu^{2+} и Fe^{3+} (***b***)
a: $[H_2SO_4]_0$ – 31 г/дм^3, $[Cu^{2+}]_0$ – 2 г/дм^3, $[Fe^{3+}]_0$ – 6,25 г/дм^3
b: $[H_2SO_4]_0$ – 50 г/дм^3, P_{O_2} – 0,475 МПа, τ – 240 мин

The coefficients of determination was $R^2 = 0.98$, confirming the adequacy of the model.

To identify statistically significant parameters and evaluate their effect on pyrite oxidation, a Pareto chart was constructed (Fig. 7).

The most influential factors are leaching time, oxygen pressure, and solution acidity. The addition of Cu^{2+} and Fe^{3+} ions has only a limited effect on oxidation efficiency, as indicated by the small change in the degree of oxidation when their concentrations are varied within the studied range.

These findings are consistent with [15], where a direct correlation was established between leaching time, oxygen pressure, and pyrite decomposition. At the same time, pyrite oxidation is accompanied by the formation of ferrous sulfate via reactions (6) and (7).

The dependence of iron leaching from pyrite on oxygen pressure and leaching time is presented in Fig. 8. At oxygen pressures below 0.5 MPa and leaching times of 60—120 min, pyrite oxidation does not exceed 35—40 %. A marked increase to 50 % is observed at $P_{O_2} = 0.75$ and $\tau = 240$ min. A nonlinear relationship between oxidation efficiency and acidity was also identified: increasing the sulfuric acid concentration from 10 to 35 g/dm^3 promoted pyrite decomposition.

Fig. 8, *b* shows the dependence of pyrite oxidation on the initial Cu^{2+} and Fe^{3+} concentrations. Introducing Fe^{3+} in the range 2.5—10.0 g/dm^3 markedly enhances pyrite oxidation, increasing the oxidation degree by ~10 % after 240 min. Pyrite is oxidized by Fe^{3+} ions, while the resulting Fe^{2+} is regenerated via reaction (10). According to the literature [28], Cu^{2+} ions exert a catalytic effect on the oxidation of Fe^{2+} to Fe^{3+}, which explains the synergistic effect observed when both ions are present. Adding Cu^{2+} at concentrations up to 2 g/dm^3 significantly accelerates Fe^{2+} oxidation to Fe^{3+}, thereby promoting further pyrite decomposition.

Optimal parameters were obtained at $P_{O_2} = 0.75$ MPa, $[H_2SO_4]_0 = 50$ g/dm^3, $[Cu^{2+}]_0 = 1.5 \div 2.0$ g/dm^3, and $[Fe^{3+}]_0 = 8 \div 10$ g/dm^3. Under these conditions, the maximum degree of pyrite oxidation reached 56 %.

From the experimental data, the following regression equation was derived:

$$Fe_2S = 38.4072 - 4.76472P_{O_2} + 0.513402C_{H_2SO_4} - 0.52213C_{Fe(III)} + 6.56917C_{Cu(II)} - 0.0712372\tau + 0.271903\,P^2_{O_2} - 0.0117899C^2_{H_2SO_4} - 0.0466268C^2_{Fe(III)} - 1.69325C^2_{Cu(II)} + 0.0000383004\tau^2. \quad (15)$$

with a coefficient of determination of $R^2 = 0.96$, confirming the adequacy of the model.

SEM images and EDS mapping of residues from low-temperature oxidation of chalcopyrite and pyrite are presented in Figs. 9 and 10. The residues were obtained at t = 100 °C, P_{O_2} = 0.75 MPa, $[H_2SO_4]_0$ = = 50 g/dm^3, $[Cu^{2+}]_0$ = 3 g/dm^3, $[Fe^{3+}]_0$ = 10 g/dm^3, τ = 240 min.

As seen in Fig. 9, chalcopyrite leach residue particles exhibit a heterogeneous surface, combining smooth areas with porous zones. EDS mapping showed the following distribution of the main components: sulfur (red), iron (green), and copper (yellow). Particles containing these zones correspond to chalcopyrite. Bright red surface deposits indicate local accumulation of elemental sulfur on chalcopyrite.

Similar studies of pyrite residues (Fig. 10) revealed a comparable but not identical pattern of surface transformations. A clear correlation was observed between particle size and composition: fine fractions consisted almost entirely of elemental sulfur, whereas larger particles corresponded to pyrite. Sulfur deposits were also detected at surface defect sites. Irregularly shaped conglomerates were especially evident on particles with developed surface morphology.

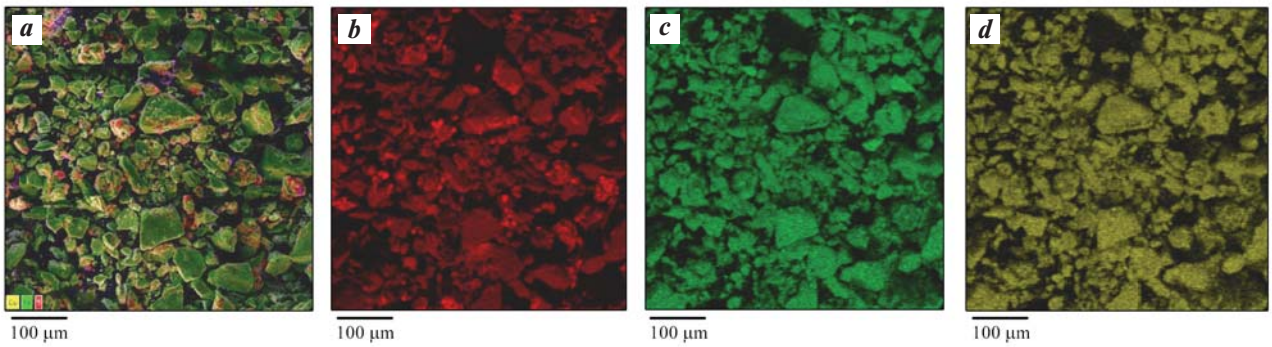

Fig. 9. SEM images of chalcopyrite oxidation residue and EDS mapping
a – general view, ***b*** – sulfur, ***c*** – iron, ***d*** – copper

Рис. 9. СЭМ-изображения частиц кека окисления халькопирита и результаты ЭДС-картирования
a – общий вид, ***b*** – сера, ***c*** – железо, ***d*** – медь

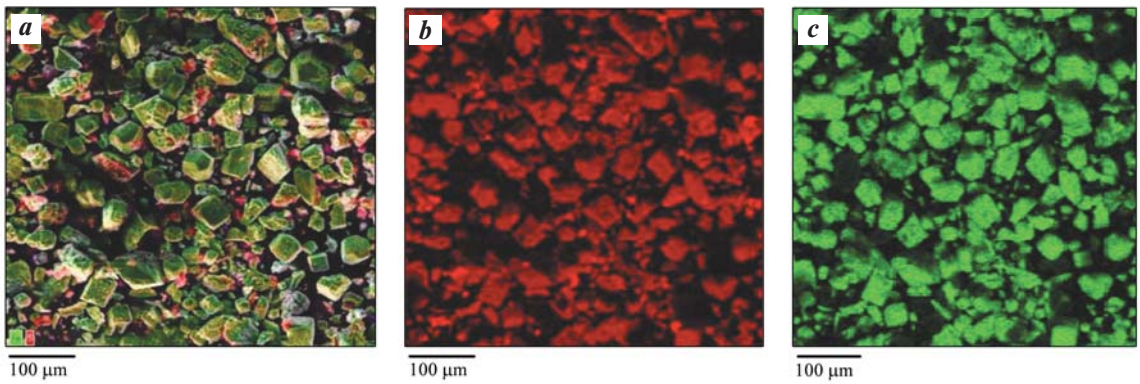

Fig. 10. SEM images of pyrite oxidation residue and EDS mapping
a – general view, ***b*** – sulphur, ***c*** – iron

Рис. 10. СЭМ-изображения частиц кека окисления пирита и результаты ЭДС-картирования
a – общий вид, ***b*** – сера, ***c*** – железо

Conclusion

This study investigated the low-temperature autoclave oxidation of the sulfide minerals, namely chalcopyrite and pyrite. Mathematical models were developed to describe the effects of oxygen pressure, sulfuric acid concentration, copper and iron ion concentrations, and leaching time, with coefficients of determination of $R^2 = 0.98$ for chalcopyrite and $R^2 = 0.96$ for pyrite, confirming the adequacy of the models. Optimal technological parameters were identified for effective decomposition of chalcopyrite, yielding 55 % copper recovery (P_{O_2} = 0.25 MPa; initial concentrations: $[H_2SO_4]_0$ = = 50 g/dm^3, $[Cu^{2+}]_0$ = 1 g/dm^3, $[Fe^{3+}]_0$ = 2.5 g/dm^3; τ = 240 min), and for pyrite, yielding 56 % iron recovery (P_{O_2} = 0.75 MPa; $[H_2SO_4]_0$ = 50 g/dm^3, $[Cu^{2+}]_0$ = = 2 g/dm^3, $[Fe^{3+}]_0$ = 10 g/dm^3; τ = 240 min).

The role of catalytic additives was also examined. Variation of the initial concentrations of $[Cu^{2+}]_0$ (1—3 g/dm^3) and $[Fe^{3+}]_0$ (2.5—10.0 g/dm^3) increased the degree of chalcopyrite oxidation by 8—11 % and pyrite oxidation by 10—13 %. SEM analysis of residues revealed local accumulation of elemental sulfur on the particle surfaces.

References

1. Shaibakova L. F. Global and Russian trends in the innovative development of copper production. *Regional'naya ekonomika i upravlenie: Elektronnyi nauchnyi zhurnal*. 2018;3(55):5. (In Russ.).
Шайбакова Л.Ф. Мировые и российские тенденции инновационного развития производства меди. *Региональная экономика и управление: Электронный научный журнал*. 2018;3(55):5.
2. Kondratiev V.B. Base metals: prospects in 2021. *Gornaya promishlennost'*. 2021;1:14—22. (In Russ.).
https://doi.org/10.30686/1609-9192-2021-1-14-22
Кондратьев В.Б. Базовые металлы: Перспективы в 2021 г. *Горная промышленность*. 2021;1:14—22.
https://doi.org/10.30686/1609-9192-2021-1-14-22
3. Vira D.Yu. Prospects for the development of Russian copper industry markets under new conditions. *Vestnik Altayskoy akademii ekonomiki i prava*. 2024;3(3):344—354. (In Russ.). https://doi.org/10.17513/vaael.3354
Вира Д.Ю. Перспективы развития рынков медной промышленности России в новых условиях. *Вестник Алтайской академии экономики и права*. 2024;3(3):344—354.
https://doi.org/10.17513/vaael.3354
4. Khopunov E.A. Modern directions of mineral raw materials processing. *Natsional'naya Assotsiatsiya Uchenykh (NAU)*. 2015;4-7(9):89—92. (In Russ.).
Хопунов Э.А. Современные направления переработки минерального сырья. *Национальная Ассоциация Ученых (НАУ)*. 2015;4-7(9):89—92.
5. Chanturia V.A., Shadrunova I.V., Gorlova O.E., Kolodezhnaya E.V. Development of technological innovations for deep and complex processing of man-made raw materials in the context of new economic challenges. *Izvestiya Tulskogo gosudarstvennogo universiteta. Nauki o zemle*. 2020;1:159—171. (In Russ.).
https://doi.org/10.46689/2218-5194-2020-1-1-159-171
Чантурия В.А., Шадрунова И.В., Горлова О.Е., Колодежная Е.В. Развитие технологических инноваций глубокой и комплексной переработки техногенного сырья в условиях новых экономических вызовов. *Известия Тульского государственного университета. Науки о земле*. 2020;1:159—171.
https://doi.org/10.46689/2218-5194-2020-1-1-159-171
6. Shumskaya E.N., Poperechnikova O.Yu., Tikhonov N.O. Development of technology for processing refractory pyrite polymetallic ore of Korbakhinskoye deposit. *Gornyy zhurnal*. 2014;(11):78—83. (In Russ.).
Шумская Е.Н., Поперечникова О.Ю., Тихонов Н.О. Разработка технологии обогащения труднообогатимой колчеданной полиметаллической руды Корбалихинского месторождения. *Горный журнал*. 2014;(11):78—83.
7. Shneerson Ya.M., Naboychenko S.S. Trends in the development of autoclave hydrometallurgy of nonferrous metals. *Tsvetnye metally*. 2011;(3):15—20. (In Russ.).
Шнеерсон Я.М., Набойченко С.С. Тенденции развития автоклавной гидрометаллургии цветных металлов. *Цветные металлы*. 2011;(3):15—20.
8. Lapshin D.A., Shneerson Ya.M. Autoclave processes in platinum metals hydrometallurgy. *Tsvetnye metally*. 2014;(5):39—43. (In Russ.).
Лапшин Д.А., Шнеерсон Я.М. Автоклавные процессы в гидрометаллургии платиновых металлов. *Цветные металлы*. 2014;(5):39—43.
9. Lapin A.Yu. History of development and implementation of autoclave-hydrometallurgical technology for processing nickel-pyrrhotite concentrates. *Tsvetnye metally*. 2020;(9):57—64. (In Russ.).
Лапин А.Ю. История создания и освоения автоклавно-гидрометаллургической технологии по пе-

переработке никель-пирротиновых концентратов. *Цветные металлы*. 2020;(9):57—64.

10. Padilla R., Vega D., Ruiz M.C. Pressure leaching of sulfidized chalcopyrite in sulfuric acid-oxygen media. *Hydrometallurgy*. 2007;86(1-2):80—88. https://doi.org/10.1016/j.hydromet.2006.10.006
11. McDonald R.G., Muir D.M. Pressure oxidation leaching of chalcopyrite. Part I. Comparison of high and low temperature reaction kinetics and products. *Hydrometallurgy*. 2007;86(3-4):191—205. https://doi.org/10.1016/j.hydromet.2006.11.015
12. Rusanen L., Aromaa J., Forsen O. Pressure oxidation of pyrite-arsenopyrite refractory gold concentrate. *Physicochemical Problems of Mineral Processing*. 2013;49:101—109. https://doi.org/10.5277/ppmp130110
13. Shoppert A., Valeev D., Loginova I., Pankratov D. Low-temperature treatment of boehmitic bauxite using the Bayer reductive method with the formation of high-iron magnetite concentrate. *Materials*. 2023;16(13):4678. https://doi.org/10.3390/ma16134678
14. Vasilyeva A.A., Boduen A.Ya., Vasilyev R.E. Analysis of the possibility of using hydrometallurgical methods to improve copper concentrate processing. *Vestnik IrGTU*. 2022;26(2):320—335. (In Russ.).
Васильева А.А., Бодуэн А.Я., Васильев Р.Е. Анализ возможности применения гидрометаллургических методов с целью улучшения переработки медных концентратов. *Вестник ИрГТУ*. 2022;26(2):320—335.
15. Epiforov A.V., Nabiulin R.N., Balikov S.V. Low-temperature autoclave oxidation of refractory sulfide gold-copper flotation concentrates followed by sulfite leaching of precious metals from oxidized cakes. *Izvestiya vuzov. Prikladnaya khimiya i biotekhnologiya*. 2014;3(8):31—38. (In Russ.).
Епифоров А.В., Набиулин Р.Н., Баликов С.В. Низкотемпературное автоклавное окисление упорных сульфидных золото-медных флотоконцентратов с последующим сульфитным выщелачиванием драгоценных металлов из окисленных кеков. *Известия вузов. Прикладная химия и биотехнология*. 2014;3(8):31—38.
16. Rogozhnikov D.A., Zakharian S.V., Dizer O.A., Karimov K.A. Nitric acid leaching of the copper-bearing arsenic sulphide concentrate of Akzhal. *Tsvetnye Metally*. 2020;8:11—16. https://doi.org/10.17580/tsm.2020.08.02
17. Gordeev D.V., Petrov G.V., Nikitina T.Yu. Application of two-stage sulfuric and chloride leaching for processing sulfide polymetallic concentrates. *Vestnik Magnitogorskogo gosudarstvennogo universiteta imeni G.I. Nosova*. 2022;20(3):13—25. (In Russ.).
Гордеев Д.В., Петров Г.В., Никитина Т.Ю. Применение двухстадийного сернокислого и хлоридного выщелачивания для переработки сульфидных полиметаллических концентратов. *Вестник Магнитогорского государственного университета им. Г.И. Носова*. 2022;20(3):13—25.
18. Rasskazova A.V., Sekisov A.G., Rasskazov M.I. Nitric-nitrite oxidation of copper-porphyry ores followed by activation chloride-sulfuric acid leaching of copper and noble metals. *GIAB*. 2023;9:130—140. (In Russ.).
Рассказова А.В., Секисов А.Г., Рассказов М.И. Азотнокислотно-нитритное окисление медно-порфировых руд с последующим активационным хлоридносернокислотным выщелачиванием меди и благородных металлов. *ГИАБ*. 2023;9:130—140.
19. Córdoba E.M., Muñoz J.A., Blázquez M.L., González F., Ballester A. Leaching of chalcopyrite with ferric ion. Part I: General aspects. *Hydrometallurgy*. 2008;93(3-4):81-87. https://doi.org/10.1016/j.hydromet.2008.04.015
20. Nourmohamadi H., Esrafili M.D., Aghazadeh V., Rezai B. The influence of Ag^{+} cation on elemental sulfur passive layer and adsorption behavior of chalcopyrite toward Fe^{3+} and Fe^{2+} ions: Insights from DFT calculations and molecular dynamics simulations. *Physica B: Condensed Matter*. 2022;627:413611. https://doi.org/10.1016/j.physb.2021.413611
21. Fomchenko N.V., Muravyov M.I. Effect of sulfide mineral content in copper-zinc concentrates on the rate of leaching of non-ferrous metals by biogenic ferric iron. *Hydrometallurgy*. 2019;185:82—87. https://doi.org/10.1016/j.hydromet.2019.02.002
22. Dizer O., Rogozhnikov D., Karimov K., Kuzas E., Suntsov A. Nitric acid dissolution of tennantite, chalcopyrite and sphalerite in the presence of Fe(III) ions and FeS_2. *Materials*. 2022;15(4):1545. https://doi.org/10.3390/ma15041545
23. Rogozhnikov D., Karimov K., Shoppert A., Dizer O., Naboichenko S. Kinetics and mechanism of arsenopyrite leaching in nitric acid solutions in the presence of pyrite and Fe(III) ions. *Hydrometallurgy*. 2021;199:105525. https://doi.org/10.1016/j.hydromet.2020.105525
24. Vasilyev V.I. Titrimetric and gravimetric methods of analysis: Textbook for university students. Moscow: Drofa, 2005. 366 p. (In Russ.).
Васильев В.И. Титриметрические и гравиметриче-

ские методы анализа: Учебник для студентов вузов. М.: Дрофа, 2005. 366 с.

25. Shneerson Ya.M., Frumina L.M., Ivanovsky V.V., Kasatkin S.V. Kinetics of oxidative pressure leaching of copper sulfide minerals. Sbornik nauchnih trudov instituta Gipronickel, Leningrad: Gipronickel, 1981. P. 53–61. (In Russ.).
Шнеерсон Я.М., Фрумина Л.М., Ивановский В.В., Касаткин С.В. Кинетика окислительного автоклавного выщелачивания медных сульфидных минералов. *Сборник научных трудов института Гипроникель*. Л.: Гипроникель, 1981. С. 53—61.
26. Córdoba E.M., Muñoz J.A., Blázquez M.L., González F., Ballester A. Leaching of chalcopyrite with ferric ion. Part IV: The role of redox potential in the presence of mesophilic and thermophilic bacteria. *Hydrometallurgy*. 2008;93(3-4):106—115. https://doi.org/10.1016/j.hydromet.2007.11.005
27. Li Y., Kawashima N., Li J., Chandra A.P., Gerson A.R. A review of the structure, and fundamental mechanisms and kinetics of the leaching of chalcopyrite. *Advances in Colloid and Interface Science*. 2013;(197-198):1—32. https://doi.org/10.1016/j.cis.2013.03.004
28. Michael J. Nicol. A comparative study of the kinetics of the oxidation of iron (II) by oxygen in acidic media — mechanistic and practical implications. *Hydrometallurgy*. 2020;192:105246. https://doi.org/10.1016/j.hydromet.2020.105246

Information about the authors

Maksim A. Tretiak – Cand. Sci. (Eng.), Junior Researcher, Scientific laboratory of advanced technologies for complex processing of mineral and man-made raw materials of non-ferrous and ferrous metals, Ural Federal University n.a. the First President of Russia B.N. Yeltsin (UrFU).
https://orcid.org/0000-0001-8405-8100
E-mail: m.a.tretiak@urfu.ru

Kirill A. Karimov – Cand. Sci. (Eng.), Senior Researcher, Scientific laboratory of advanced technologies for complex processing of mineral and man-made raw materials of non-ferrous and ferrous metals, UrFU.
https://orcid.org/0000-0003-1415-4484
E-mail: k.a.karimov@urfu.ru

Ulyana R. Sharipova – Master's Student, Research Engineer, Scientific laboratory of advanced technologies for complex processing of mineral and man-made raw materials of non-ferrous and ferrous metals, UrFU.
https://orcid.org/0000-0003-2598-8046
E-mail: ursharipova@urfu.ru

Aleksey V. Kritsky – Cand. Sci. (Eng.) Researcher, Scientific laboratory of advanced technologies for complex processing of mineral and man-made raw materials of non-ferrous and ferrous metals, UrFU.
https://orcid.org/0000-0002-8575-5925
E-mail: a.v.kritsky@urfu.ru

Denis A. Rogozhnikov – Dr. Sci. (Eng.), Head of the Scientific laboratory of perspective technologies for complex processing of mineral and man-made raw materials of non-ferrous and ferrous metals, UrFU.
https://orcid.org/0000-0002-5940-040X
E-mail: darogozhnikov@urfu.ru

Информация об авторах

Максим Алексеевич Третьяк – к.т.н., мл. науч. сотрудник научной лаборатории перспективных технологий комплексной переработки минерального и техногенного сырья цветных и черных металлов, Уральский федеральный университет имени первого Президента России Б.Н. Ельцина (УрФУ).
https://orcid.org/0000-0001-8405-8100
E-mail: m.a.tretiak@urfu.ru

Кирилл Ахтямович Каримов – к.т.н., ст. науч. сотрудник научной лаборатории перспективных технологий комплексной переработки минерального и техногенного сырья цветных и черных металлов, УрФУ.
https://orcid.org/0000-0003-1415-4484
E-mail: k.a.karimov@urfu.ru

Ульяна Рамильевна Шарипова – магистрант УрФУ, инженер-исследователь научной лаборатории перспективных технологий комплексной переработки минерального и техногенного сырья цветных и черных металлов, УрФУ.
https://orcid.org/0000-0003-2598-8046
E-mail: ursharipova@urfu.ru

Алексей Владимирович Крицкий – к.т.н., науч. сотрудник научной лаборатории перспективных технологий комплексной переработки минерального и техногенного сырья цветных и черных металлов, УрФУ.
https://orcid.org/0000-0002-8575-5925
E-mail: a.v.kritsky@urfu.ru

Денис Александрович Рогожников – д.т.н., зав. лабораторией перспективных технологий комплексной переработки минерального и техногенного сырья цветных и черных металлов, УрФУ.
https://orcid.org/0000-0002-5940-040X
E-mail: darogozhnikov@urfu.ru

Contribution of the authors

M.A. Tretiak – defined the research objectives and plan, conducted the first-stage experiments, processed the results, and prepared the article materials.

K.A. Karimov – supervised and monitored the progress of the work, participated in the discussion of the results, and contributed to the preparation of the article materials.

U.R. Sharipova – processed the results, prepared the article materials and documentation.

A.V. Kritskiy – conducted the second-stage experiments and participated in the discussion of the results.

D.A. Rogozhnikov – supervised and monitored the progress of the work and participated in the discussion of the results.

Вклад авторов

М.А. Третьяк – определение цели и плана работы, проведение экспериментов первого этапа, обработка результатов, подготовка материалов статьи.

К.А. Каримов – курирование и контроль хода работы, участие в обсуждении результатов, подготовка материалов статьи.

У.Р. Шарипова – обработка результатов, подготовка материалов статьи и документации.

А.В. Крицкий – проведение экспериментов второго этапа, участие в обсуждении результатов.

Д.А. Рогожников – курирование и контроль хода работы, участие в обсуждении результатов.

The article was submitted 05.05.2025, revised 19.05.2025, accepted for publication 23.05.2025

Статья поступила в редакцию 05.05.2025, доработана 19.05.2025, подписана в печать 23.05.2025